

INERTIA FLOW OF VISCOPLASTIC FLUIDS APPROXIMATED BY A MULTI-FIELD STABILIZED METHOD

Lober Hermany, hermany@mecanica.ufrgs.br

Daniel Dall'Onder dos Santos, dallonder@mecanica.ufrgs.br

Sérgio Frey, frey@mecanica.ufrgs.br

Laboratory of Computational and Applied Fluid Mechanics (LAMAC), Department of Mechanical Engineering, Universidade Federal do Rio Grande do Sul, Rua Sarmento Leite, 425, 90050-170, Porto Alegre, RS, Brazil

Mônica F. Naccache, naccache@mec.puc-rio.br*

Paulo R. de Souza Mendes, pmendes@mec.puc-rio.br*

Department of Mechanical Engineering, Pontifícia Universidade Católica-RJ, Rua Marquês de São Vicente 225, Rio de Janeiro, RJ 22453-900, Brazil

***Abstract.** The effect of inertia in the flow of viscoplastic fluids through an expansion followed by a contraction is analyzed. The mechanical behavior is modeled by the Generalized Newtonian Fluid constitutive equation, with the viscosity function given by the SMD equation (de Souza Mendes and Dutra, 2004). The conservation equations of mass and momentum, together with the constitutive equation are approximated by a Galerkin least-squares (GLS) formulation in terms of pressure and velocity. A sensitivity analysis is performed, aiming at investigating the influence of inertia and viscous forces on the fluid dynamics. The topology of yield surfaces is obtained, and proved to be strongly related to inertia and yield stress amounts considered in the flow. Moreover, the results are compared to other results from the literature, which consider fluid elasticity. It is observed that inertia and elasticity effects lead to different flow patterns.*

***Keywords:** SMD model, Galerkin Least-Squares method, shear-thinning viscoplastic flow, viscoplastic inertial flows.*

1. INTRODUCTION

This paper presents numerical results of inertial flow of viscoplastic fluids through an abrupt expansion followed by a contraction in an axisymmetric channel. Viscoplastic fluids are present in several important industrial processes. In the petroleum industry, for example, the drilling fluid of the wells are viscoplastic materials. Several other examples can be found in food and cosmetics. There are also paints, pharmaceuticals, and biological fluids which present a mechanical behavior of a fluid viscoplastic. The pattern of these flows is characterized by two distinct regions: the unyielded regions where the stresses are less than the elastic limit stress and strain is extremely low, and the yielded regions, which appear where the stress level is higher than the yield stress. The topology of the zones define some important characteristics of the flow, as the amount of fluid that may remain stagnant in a specific region of the flow or pressure drop along this flow. Therefore, the study of the pattern of flow and determining how it is affected by the parameters ruling is of great interest. The main focus of this paper is to present numerical results of the effects of inertia in a complex geometry. And therefore analyze the influence of rheological and kinematic parameters that govern the flow, the morphology of the rigid zones of viscoplastic fluid flow through an expansion followed by an abrupt contraction in an axisymmetric duct.

The mixed Galerkin least-squares (GLS) approximations for viscoplastic flows is performed in this article. The selected model is the Souza Mendes and Dutra model – or simply SMD model – introduced by Souza Mendes and Dutra (2004). This GLS methodology – introduced by Hughes *et al.* (1986) for the Stokes problem, was later extended to mixed Navier-Stokes equations in Franca and Frey (1992) and multi-field Navier-Stokes equations in Behr *et al.* (1993). It does not need to satisfy the compatibility condition arisen from finite element sub-spaces for the pair pressure–velocity – the known Babuška-Brezzi condition. This is accomplished by adding mesh-dependent terms which are functions of residuals of the flow governing equations, evaluated element-wise. In this way, the compatibility condition may be circumvented and the methodology still remains stable – employing simple combinations of equal-order finite element interpolations.

The numerical solution of steady flows of SMD fluids on an axisymmetric expansion-contraction is obtained and compared with some results from the literature. The viscoplastic effects are evaluated for a dimensionless flow rate (U^*) from 0.25 to 1.5; the inertia effects are evaluated for a rheological Reynolds number (Re_r) from 0.5 to 25 and the power-law index (n) from 0.4 to 1.0. All the numerical results proved to be physically meaningful and in accordance with the related literature.

2. MECHANICAL MODELING

This work considers that the fluid is incompressible in steady flow and the governing equations are expressed in a fixed Eulerian system. Let $\Omega \in \mathcal{R}^{n_{dim}}$, where n_{dim} denotes the number of spatial dimensions, being the fluid domain with boundary Γ . The continuity and momentum conservation equations, with the imposed boundary conditions, can be respectively expressed as:

$$\begin{aligned} \rho(\nabla \mathbf{u}) \mathbf{u} &= -\nabla p + 2\eta(\dot{\gamma}) \operatorname{div} \mathbf{D}(\mathbf{u}) + \mathbf{f} && \text{in } \Omega \\ \operatorname{div} \mathbf{u} &= 0 && \text{in } \Omega \\ \mathbf{u} &= \mathbf{u}_g && \text{on } \Gamma_g^u \\ [2\eta(\dot{\gamma}) \mathbf{D}(\mathbf{u}) - p \mathbf{1}] \mathbf{n} &= \mathbf{t}_h && \text{on } \Gamma_h \end{aligned} \quad (1)$$

where \mathbf{u} is the velocity vector, p the hydrostatic pressure, ρ the fluid density, \mathbf{f} the body force vector, \mathbf{u}_g the imposed velocity boundary condition, \mathbf{t}_h the stress vector, \mathbf{D} is the strain rate tensor given by

$$\mathbf{D}(\mathbf{u}) = \frac{1}{2}(\nabla \mathbf{u} + (\nabla \mathbf{u})^T) \quad (2)$$

and $\eta(\dot{\gamma})$ is SMD viscosity function defined as

$$\eta(\dot{\gamma}) = (1 - \exp(-\eta_0 \dot{\gamma} / \tau_0)) \left(\frac{\tau_0}{\dot{\gamma}} + K (\dot{\gamma})^{n-1} \right) \quad (3)$$

where K is the consistency index, n is the power-law exponent and τ_0 is the yield stress. For stress values around the yield stress ($\tau \approx \tau_0$), the strain rate goes from $\dot{\gamma}_0 = \tau_0 / \eta_0$ (the end of the high Newtonian viscosity region), to $\dot{\gamma}_1 = (\tau_0 / K)^{1/n}$ (the beginning of the power-law viscosity region) – see, for details, de Souza Mendes *et al.* (2007) – often increasing orders of magnitude. This property, amongst round-off errors during the numerical computations, can lead to a troublesome determination of the location where the material “actually” begins to flow – see, for more discussion, Santos *et al.* (2011).

In order to obtain the dimensionless governing parameters, the rheological dimensionless normalization introduced by de Souza Mendes (2007) is applied. Therefore the following set of dimensionless quantities are introduced:

$$\mathbf{x}^* = \frac{\mathbf{x}}{L_c}; \quad \mathbf{u}^* = \frac{\mathbf{u}}{\dot{\gamma}_c L_c}; \quad p^* = \frac{p}{\tau_0}; \quad \boldsymbol{\tau}^* = \frac{\boldsymbol{\tau}}{\tau_0}; \quad \mathbf{f}^* = \frac{L_c \mathbf{f}}{\tau_0} \quad (4)$$

where $\dot{\gamma}_c$ is the characteristic strain rate of the flow and L_c is the characteristic length – in this work taken equal to $\dot{\gamma}_1$ and r (the main tube radius, see Fig. 1), respectively.

Hence, substituting the dimensionless variables introduced above into the boundary value problem given by Eq. (1), the dimensionless mixed formulation for inertia flows of SMD fluids is given by:

$$\begin{aligned} Re_r (\nabla^* \mathbf{u}^*) \mathbf{u}^* + \nabla^* p^* - 2\eta^*(\dot{\gamma}^*) \operatorname{div}^* \mathbf{D}(\mathbf{u}^*) &= \mathbf{f}^* && \text{in } \Omega^* \\ \operatorname{div}^* \mathbf{u}^* &= 0 && \text{in } \Omega^* \\ \mathbf{u}^* &= \frac{\mathbf{u}_g}{\dot{\gamma}_1 L_c} && \text{on } \Gamma_g^{u^*} \\ [2\eta^*(\dot{\gamma}^*) \mathbf{D}(\mathbf{u}^*) - p^* \mathbf{1}] \mathbf{n} &= \mathbf{t}_h^* && \text{on } \Gamma_h^* \end{aligned} \quad (5)$$

where Re_r is the rheological version for the Reynolds number given by

$$Re_r = \frac{\rho(\dot{\gamma}_1 L_c) L_c}{\eta(\dot{\gamma}_1)} = \frac{\rho(\dot{\gamma}_1 L_c) L_c}{2K \dot{\gamma}_1^{n-1}} = \frac{\rho}{2K \dot{\gamma}_1^{n-2} L^{-2}} \quad (6)$$

For SMD fluid flows, the Reynolds number usually employed in the literature is related to the rheological Reynolds number as $Re = 2Re_r U^{*(2-n)}$.

Remark: The rheological Reynolds number defined by Eq. (6) is a dimensionless group based only on the rheological fluid properties, and, therefore, entirely uncoupled of the flow kinematics as it uses to be. Souza Mendes (2007) suggests this definition claiming that Re_r may be viewed as a dimensionless fluid density.

3. THE FINITE ELEMENT APPROXIMATION

Based on usual definitions of finite element sub-spaces for pressure (P^h) and velocity (\mathbf{V}^h) (see, for instance Franca and Frey (1992)), a GLS formulation for SMD fluid flows may be written as: *find the pair* $(p^h, \mathbf{u}^h; q^h, \mathbf{v}^h) \in P^h \times \mathbf{V}_g^h$ *such that*

$$\begin{aligned}
 & + \int_{\Omega} \rho ([\nabla \mathbf{u}^h] \mathbf{u}^h) \cdot \mathbf{v}^h d\Omega + 2\eta(\dot{\gamma}) \int_{\Omega} \mathbf{D}(\mathbf{u}^h) \cdot \mathbf{D}(\mathbf{v}^h) d\Omega - \int_{\Omega} p^h \operatorname{div} \mathbf{v}^h d\Omega + \int_{\Omega} \operatorname{div} \mathbf{u}^h q^h d\Omega \\
 & + \int_{\Omega} \operatorname{div} \mathbf{u}^h \delta(Re_K) \operatorname{div} \mathbf{v}^h d\Omega + \epsilon \int_{\Omega} p^h q^h d\Omega \\
 & + \sum_{K \in \Omega^h} \int_{\Omega_K} (\rho [\nabla \mathbf{u}^h] \mathbf{u}^h + \nabla p^h - 2\eta(\dot{\gamma}) \operatorname{div} \mathbf{D}(\mathbf{u}^h)) \cdot (\alpha(Re_K)(\rho [\nabla \mathbf{v}^h] \mathbf{u}^h + \nabla q^h - 2\eta(\dot{\gamma}) \operatorname{div} \mathbf{D}(\mathbf{v}^h))) d\Omega \quad (7) \\
 & = \int_{\Omega} \mathbf{f} \cdot \mathbf{v}^h d\Omega + \int_{\Gamma_h} \mathbf{t}_h \cdot \mathbf{v}^h d\Gamma \\
 & + \sum_{K \in \Omega^h} \int_{\Omega_K} \mathbf{f} \cdot (\alpha(Re_K)(\rho [\nabla \mathbf{v}^h] \mathbf{u}^h + \nabla q^h - 2\eta(\dot{\gamma}) \operatorname{div} \mathbf{D}(\mathbf{v}^h))) d\Omega, \quad \forall (q^h, \mathbf{v}^h) \in P^h \times \mathbf{V}_g^h
 \end{aligned}$$

where Re_{r_K} denotes the grid rheological Reynolds number, $\alpha(Re_{r_K})$ and β are the stability parameters for the motion and continuity equations, respectively – see Franca and Frey (1992) for their definitions.

4. NUMERICAL RESULTS

The GLS approximation for SMD fluids (Eq.(7)) is employed to simulate the flow over an abrupt expansion followed by an abrupt contraction. Fig. 1 shows the geometry and a blown-up view of the employed mesh. The geometry is very similar to the ones used by Naccache and Barbosa (2007) and de Souza Mendes *et al.* (2007). After a mesh independence test procedure, based on an acceptable error of 2% of the stress modulus value on the tube wall, the computational domain Ω^h is partitioned by 10,500 equal-order Lagrangian bi-linear (Q1) finite elements, rendering a total of 32,523 degrees-of-freedom. The smallest dimensionless mesh size, $h_{K^* \min} = h_K/H$, is equal to 0.099. The geometry lengths are: $R_2=6.3$ m, $R_1=1.0$ m, $L_2=6.3$ m and $L_1=18.85$ m. The boundary conditions employed are impermeability and non-slip on the main tube and on the expansion-contraction walls, fully-developed profiles for velocity at the inflow and outflow of the tube and symmetry on the tube centerline ($u_2=0$).

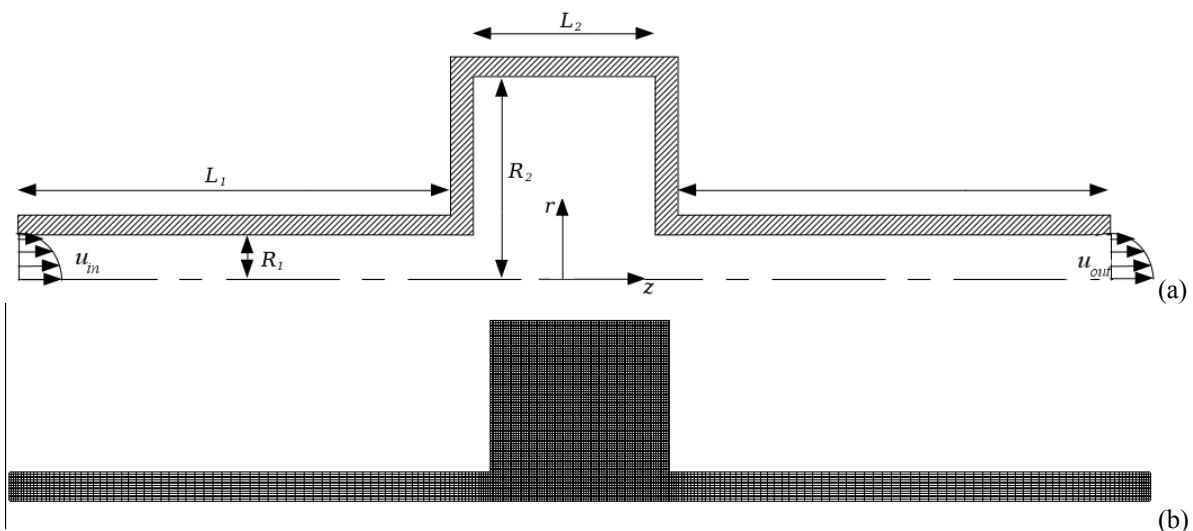


Figure 1. Flow over an abrupt expansion-contraction: (a) problem statement; (b) a mesh detail.

Figure 2 show the unyielded regions for inertia flows with $Re_r=25$, $J=18000$, $n=0.4$ and the dimensionless flow rate ranging from 0.25 to 1.50.. It can be observed that the unyielded regions upstream and downstream the expansion-contraction are symmetric for low values of U^* – performing a rigid body motion – plug flow – along the upstream and downstream tubes. The zone on the top of the cavity, where the fluid is almost quiescent, also presents a symmetric pattern. When the dimensionless flow rate is increased, the symmetry is broken: the unyielded region on the upstream tube is slightly reduced on Fig. 2b, while the unyielded regions on the upstream tube completely vanishes on Fig. 2c and

Fig 2d. Once the inertia effects are present, the upwind behavior of the velocity entails higher strain rates after the contraction, implying also on higher stress levels on the region, exceeding the yield-stress. The symmetry of the unyielded zone on the top of the expansion-contraction is also broken – as can be noticed comparing Figs. 2a and 2d – as well as its shape is reduced. The island on the geometry centerline also is reduced and is slightly carried downstream.

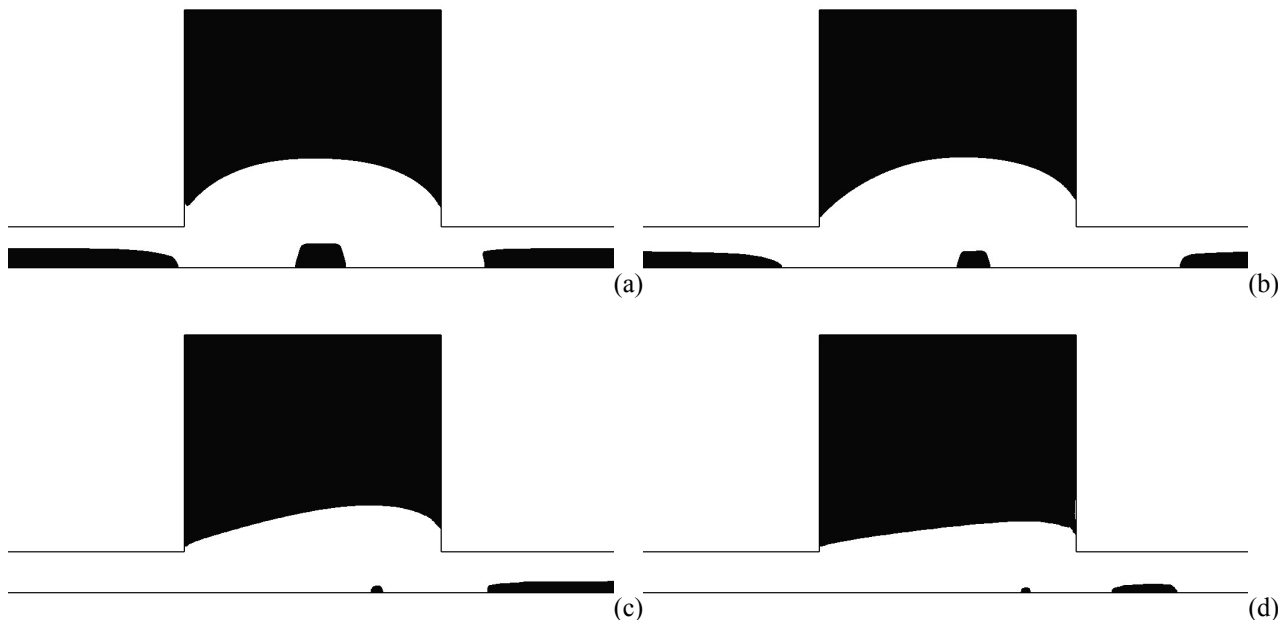
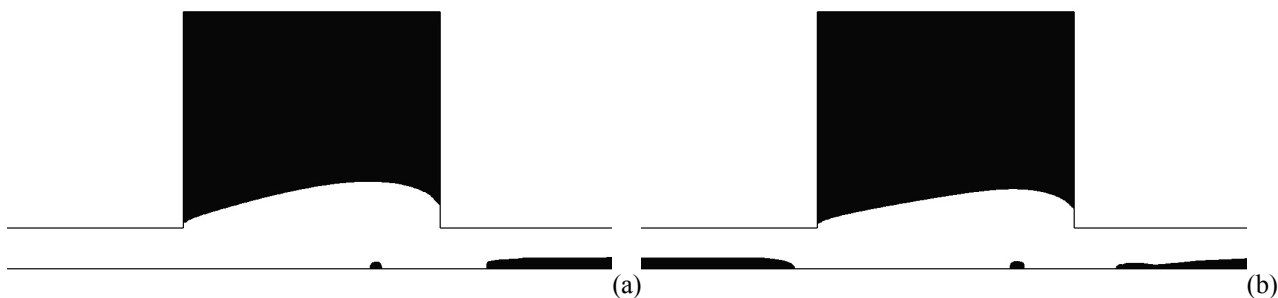


Figure 2. Morphology of the yielded regions for $Re_r=25$, $J=18000$, $n=0.4$: (a) $U^*=0.25$; (b) $U^*=0.50$; (c) $U^*=1.00$; (d) $U^*=1.50$.

Figure 3 show the unyielded regions for inertia flows with $Re_r=25$, $J=18000$, $U^*=1.0$ and power-law index ranging from 0.4 to 1.0. One may observe that the unyielded regions upstream and downstream the expansion-contraction are reduced in thickness – with a small elongation on the longitudinal direction – with the increasing of the power-law index. In the other hand, the unyielded region inside the expansion-contraction, as well as the island on the geometry center at the tube centerline, are increased with the increase of the power-law index. This difference on the behavior exists once the main tube presents predominantly $\dot{\gamma} > 1$, while the other regions presents $\dot{\gamma} < 1$. With the aid of Fig. 4 – the SMD flow curves for $n=0.2$ and 0.8 – it is more clear to understand such kind of behavior, once is a computational issue. Increasing the power-law index, strain rates smaller than 1.0 reduces the stress value – in some regions – to values smaller than the yield-stress, and so, increases the unyielded zones.



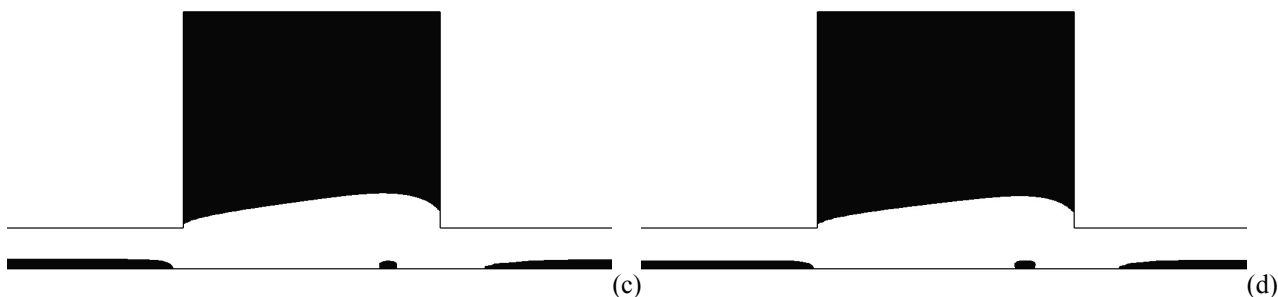


Figure 3. Morphology of the yielded regions for $Re_r=25$, $J=18000$, $U^*=1.00$: (a) $n=0.4$; (b) $n=0.6$; (c) $n=0.8$; (d) $n=1.0$.

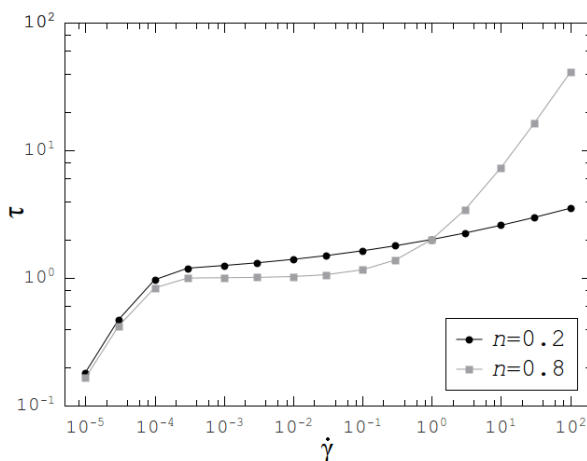
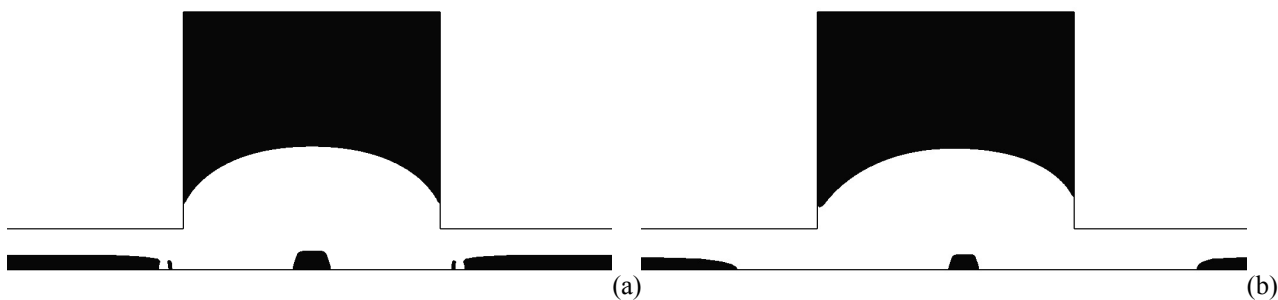


Figure 4 – SMD flow curves for $n=0.2$ and 0.8 .

The increase of the rheological Reynolds number produces an effect similar to that produced by increasing the dimensionless flow rate, that is to say, the larger the Reynolds, the greater the asymmetry of the unyielded zones. Once again it is worth mentioning that the asymmetry presented by Fig. 5 is produced by the upwind effect of the inertia term of the equation of motion. Increasing the amount of momentum, the unyielded region inside the expansion-contraction is distorted and increases in thickness. This phenomena is due to the decrease of the viscous forces acting on the flow against the increase of the inertia forces. In the same way, the island on the geometry center at the centerline is shifted to the right, with a slightly reduction on its size. It is important to emphasize that the rheological dimensionless quantities defined by Eq. (4)-(6) have fundamental importance on the investigation of the effects of inertia and viscoplasticity on the flow. Thanks to this new methodology, the amount of inertia on the flow can be increased without changing the yield-stress level of the fluid, or more specifically, in Fig. 5 is possible to increase the rheological Reynolds number, with the same dimensionless flow rate.



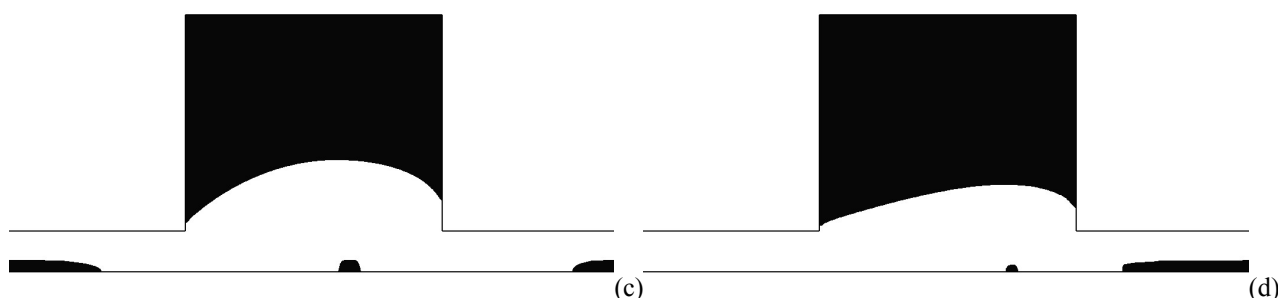


Figure 5. Morphology of the yielded regions for $U^*=1.0$, $J=18000$, $n=0.4$: (a) $Re_t=0.5$; (b) $Re_t=5.0$; (c) $Re_t=10.0$; (d) $Re_t=25.0$.

5. FINAL REMARKS

In this article, a mixed GLS approximation for the SMD constitutive model is introduced and discussed. Some numerical computations for inertia flows through an axisymmetric expansion-contraction are presented. The influence of inertia, the power-law index and the yield stress level – ranged by the dimensionless flow rate, U^* – on the unyielded zones of the fluid were presented and analyzed, with the aid a new definition of dimensionless rheological quantities. These are obtained following the definitions proposed in de Souza Mendes (2007), which allows a better analysis of the effects of inertia and viscoplasticity on the flow, since it makes possible to change the rheological Reynolds number for a fixed yield-stress level.

6. ACKNOWLEDGEMENTS

The authors L. Hermany and D. Dall'Onder dos Santos thanks for his graduate scholarship provided by CAPES and the author S. Frey, M. Naccache and P.R. De Souza Mendes acknowledges CAPES and CNPq for financial support.

7. REFERENCES

- Behr, M., Franca, L.P., Tezduyar, T.E., 1993. "Stabilized Finite Element Methods for the Velocity-Pressure-Stress Formulation of Incompressible Flows", *Comput. Methods Appl. Mech. Engrg.*, Vol.104, pp. 31-48.
- De Souza Mendes, P.R., and Dutra, E.S.S., 2004, "Viscosity Function for Yield-Stress Liquids", *Applied Rheology*, Vol. 14, pp. 296-302.
- De Souza Mendes, P.R., 2007. "Dimensionless Non-Newtonian Fluid Mechanics", *J. Non-Newtonian Fluid Mech.*, Vol.147, pp. 109-116.
- De Souza Mendes, P.R., Naccache, M. F., Vargas, P.R., and Marchesini, F.H., 2007. "Flow of viscoplastic liquids through axisymmetric expansions – contractions", *Journal of Non-Newtonian Fluid Mechanics*, vol. 142, pp. 207-217.
- Franca, L. P., Frey, S., 1992, "Stabilized Finite Element Methods: II. The Incompressible Navier-Stokes Equations", *Comput. Methods Appl. Mech. Engrg.*, 99, pp. 209-233.
- Hughes, T.J.R., Franca, L.P., Balestra, M., 1986. "A new finite element formulation for computational fluid dynamics: V. Circumventing the Babuška-Brezzi condition: A stable Petrov-Galerkin formulation of the Stokes problem accomodating equal-order interpolations", *Comput. Methods Appl. Mech. Engrg.*, Vol.59, pp. 85-99.
- Naccache M. F. , Barbosa R. S. , 2007. "Creeping flow of viscoplastic materials through a planar expansion followed by a contraction", *Mechanics Research Communications*, vol. 34 , pp. 423-431.
- Santos, D.D.O., Frey, S.L., Naccache, M.F., and Souza Mendes, P.R., 2011, "Numerical approximations for SMD flows in a lid-driven cavity", *JNNFM*, Article In Press, 2011.

8. RESPONSIBILITY NOTICE

The authors are the only responsible for the printed material included in this paper.